

Phase equilibria of hydrated Portland cement

Erik P. Nielsen^{a,*}, Duncan Herfort^a, Mette R. Geiker^b

^aAALBORG WHITE® Research and Development Centre, Aalborg Portland A/S, P.O. Box 165, DK-9100 Aalborg, Denmark

^bDepartment of Civil Engineering (Building 118), Technical University of Denmark, DK-2800 Lyngby, Denmark

Received 11 June 2003; accepted 17 May 2004

Abstract

A model is described for predicting the equilibrium phase assemblage in hydrated Portland cement and for calculating the relative contents and composition of phases present in the assemblage, from the chemical composition of the cement and the water/cement ratio. The method is also used to calculate the content of capillary pores using the best available data for the densities for each of the phases. These calculations were carried out on three different Portland cements (two white Portland cements and one grey) at water/cement ratios of 0.70. Energy dispersive spectroscopy (EDS) analysis on the SEM was used to verify the presence of all phases predicted by the model. A density for the C-S-H phase of approximately 2.10 g/cm³ and an evaporable water content in the C-S-H of approximately 19% provided the best agreement between the predicted values of chemical shrinkage, loss of ignition and content of evaporable water, and experimental data. Other results included compositional data on the C-S-H phase corresponding to molar ratios of Al/Ca=0.04 and S/Ca=0.03 in all cements investigated, and Fe/Ca=0.02 in the grey Portland cement.

© 2004 Elsevier Ltd. All rights reserved.

Keywords: Phase equilibria; Modelling; Phase rule; EDS analysis; Portland cement

1. Introduction

In Powers' model [1], the hydrated Portland cement is assumed to consist of a single hydrate phase with properties corresponding to the average of all phases present. This fails to take into account the true multiphase nature of hydrated Portland cement.

More appropriate mathematically derived models (in, e.g., Refs. [2–4]) have been used to describe the hydration of cement over time and as a function of the degree of hydration of the clinker phases. Although these models are clearly an improvement on the more simplistic Powers' model, they do not generally satisfy Gibb's Phase Rule, which applies to all chemical systems at equilibrium.

For hydrated Portland cement pastes, it is reasonable to assume that equilibrium conditions apply after two or three months of hydration because the reaction of the unhydrated clinker proceeds very slowly at this stage (e.g., Ref. [5]). The validity of this assumption is, however, dependent on

the composition of the cement and the hydraulic reactivity of the anhydrous phases, the water-to-cement ratio, the presence of supplementary cementitious materials, etc.

In the present paper, a method is described for predicting the metastable or stable phase assemblage in hydrated Portland cement systems from the chemical composition of the cement and for calculating the relative contents of phases present. The predictions were subsequently tested experimentally as part of extensive studies on concrete durability by the present authors. Parts of the model have already been described in earlier publications (e.g., Refs. [6–8]), but further development has occurred since then, and the model has been modified accordingly.

2. Phase equilibria

As noted above, the 'phase rule' applies to all chemical systems in equilibrium. Although the formulation of the rule is very simple, it has rarely been applied to hydrated cement systems (e.g., in Ref. [9]). The rule states that the number of phases plus the degrees of freedom equals the number of

* Corresponding author. Tel.: +45-98-77-76-85.

E-mail address: epn@aalborg-portland.dk (E.P. Nielsen).

components, plus a constant n , which is dependent on the history of the system with respect to pressure and temperature. If the process is kept under isobaric or isothermal conditions, n is 1, if neither, n is 2, and if both, n is 0 [10]. At constant temperature and pressure, the rule takes the form $P + F = C$.

In a fully hydrated Portland cement, which, as a first approximation, is invariant at constant temperature and pressure, the relative contents of phases of known composition present can be calculated by solving n equations for n unknowns, where n is the number of components and phases. Because the system is invariant, the composition of each of the phases must remain constant. As an example, the amount of each of the six phases in an invariant six-component system can be calculated by solving the six by six matrix in Eq. (1).

$$\begin{bmatrix} W_{C1}^{P1} & W_{C1}^{P2} & W_{C1}^{P3} & W_{C1}^{P4} & W_{C1}^{P5} & W_{C1}^{P6} \\ W_{C2}^{P1} & W_{C2}^{P2} & W_{C2}^{P3} & W_{C2}^{P4} & W_{C2}^{P5} & W_{C2}^{P6} \\ W_{C3}^{P1} & W_{C3}^{P2} & W_{C3}^{P3} & W_{C3}^{P4} & W_{C3}^{P5} & W_{C3}^{P6} \\ W_{C4}^{P1} & W_{C4}^{P2} & W_{C4}^{P3} & W_{C4}^{P4} & W_{C4}^{P5} & W_{C4}^{P6} \\ W_{C5}^{P1} & W_{C5}^{P2} & W_{C5}^{P3} & W_{C5}^{P4} & W_{C5}^{P5} & W_{C5}^{P6} \\ W_{C6}^{P1} & W_{C6}^{P2} & W_{C6}^{P3} & W_{C6}^{P4} & W_{C6}^{P5} & W_{C6}^{P6} \end{bmatrix} \begin{bmatrix} P_{1,\text{total}} \\ P_{2,\text{total}} \\ P_{3,\text{total}} \\ P_{4,\text{total}} \\ P_{5,\text{total}} \\ P_{6,\text{total}} \end{bmatrix} = \begin{bmatrix} C_{1,\text{total}} \\ C_{2,\text{total}} \\ C_{3,\text{total}} \\ C_{4,\text{total}} \\ C_{5,\text{total}} \\ C_{6,\text{total}} \end{bmatrix} \quad (1)$$

where $P_{m,\text{total}}$ is the total content of phase m in the system, in wt.%, W_{Cj}^{Pm} is the weight fraction of the component j in phase m , and $C_{j,\text{total}}$ is the total content of the component j in the system in wt.%.

A fully hydrated Portland cement paste has typically six major components (i.e., SiO_2 , Al_2O_3 , CaO , Fe_2O_3 , SO_3 , and H_2O) and can form a maximum of six phases (five hydrate phases and the pore solution) at constant temperature and pressure. For a typical Portland cement paste, these phases are assumed to be C-S-H, calcium hydroxide (CH), monosulfate ($\text{C}_3\text{A} \cdot \text{C}\bar{\text{S}} \cdot \text{H}_{12}$), ettringite ($\text{C}_3\text{A} \cdot 3\text{C}\bar{\text{S}} \cdot \text{H}_{32}$), iron oxide (probably FH_3), and pore solution.

Alkalis are disregarded in this paper, as they do not form any solid phases within the range of concentrations observed in Portland cement pastes [11]. A significant portion of the alkalis appears to be incorporated in the structure of the C-S-H, whilst remainder is present in solution at well-defined distribution ratios between the two phases [11,12]. The inclusion of alkalis in the model is described in Ref. [13].

Poor crystalline calcium silicate hydrate, C-S-H, and calcium hydroxide are the main hydrate phases in Portland cement systems, formed by the hydration of C_3S and C_2S . Different compositions of the C-S-H in Portland cement systems have been proposed, but $\text{C}_{1.75}\text{SH}_4$ appears to be the most frequently reported (in, e.g., Ref. [5,6,8]). Al and S are typically observed to be incorporated in the C-S-H,

corresponding to $\text{Al}/\text{Ca} = 0.04$ and $\text{S}/\text{Ca} = 0.03$ ([8,14]; determined by energy dispersive spectroscopy (EDS) analysis on different mature Portland cement pastes wet cured at 20°C). The density of the phase under saturated conditions has been reported at values ranging from 1.95 to 2.45 g/cm^3 [5], with most values at the lower end, and contents of evaporable water around 18–20% [5,11].

Depending on the $\text{Al}_2\text{O}_3/\text{SO}_3$ ratio [5,15,16], a hydroxy-AFm phase may replace ettringite, or gypsum may replace monosulfate, as seen on the $\text{C}_3\text{A}-\text{CaSO}_4$ binary side of the diagram for the ternary subsystem $\text{C}_3\text{A}-\text{CaSO}_4-\text{CaCO}_3$ shown in Fig. 1. For convenience, CaCO_3 , CaSO_4 , and C_3A are chosen as components rather than CO_2 , SO_3 , and Al_2O_3 . This is valid as long as these components occur as stoichiometric units in all hydrate phases. The other phases (i.e., C-S-H, CH, FH_3 , and pore solution) occur as excess phases in most assemblages formed from normal Portland cement.

If solid solution phases where the anionic substitution of, e.g., SO_4^{2-} or CO_3^{2-} in AFm or AFt phases occur in a system, these should be easily detectable by EDS analysis or similar techniques, as molar ratios of, e.g., Cl/Ca and S/Ca in such phases would change following the degree of anionic substitution. In this study, ettringite and monosulfate, when present, were invariably found as pure end-member phases. The distinction between monocarbonate, hemiacarbonate, and hydroxy-AFm phases, or a solid solution between these, is difficult to make by this method but can be performed by other methods, such as X-ray diffraction.

At ages less than about 1 year, the composition of the hydroxy-AFm is most likely to be C_4AH_{13} (e.g., in Ref. [5]) or C_4AH_{18} (e.g., in Ref. [16]), but in older pastes, the more stable phase hydrogarnet, C_3AH_6 , is likely to be present instead [5,15].

Kuzel and Pöllmann [16], who studied the $\text{CaO}-\text{Al}_2\text{O}_3-\text{CaSO}_4-\text{CaCO}_3-\text{H}_2\text{O}$ system, found that in relatively young pastes (hydrated for less than a month), the phases formed were hemiacarbonate ($\text{C}_3\text{A} \cdot 1/2\text{C}\bar{\text{C}} \cdot 1/2\text{CH} \cdot \text{H}_{11.5}$), monocarbonate ($\text{C}_3\text{A} \cdot \text{C}\bar{\text{C}} \cdot \text{H}_{12}$), monosulfate, ettringite, and calcium hydroxide. At increasing contents of CaCO_3 , the amount of monocarbonate was found to increase relative to hemiacar-

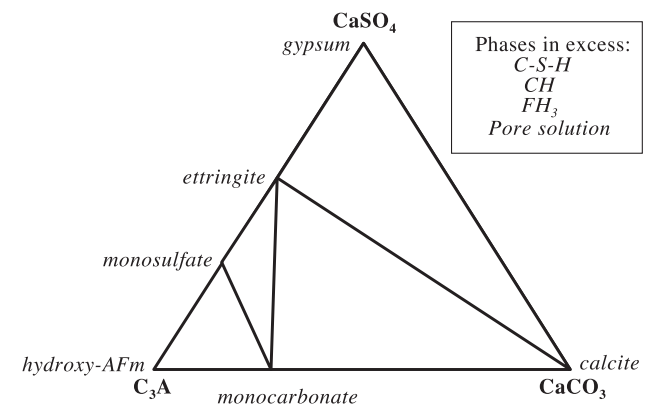


Fig. 1. Ternary subsystem $\text{C}_3\text{A}-\text{CaSO}_4-\text{CaCO}_3$ assumed for the thermodynamic model.

bonate, and the content of monosulfate was reduced. Such a phase assemblage does not satisfy the phase rule, as there is one phase too many (i.e., the solution itself is also a phase), and equilibrium conditions can therefore not apply. Damidot and Glasser [15] concluded that hem carbonate is only stable at low concentrations of carbonate and sulfate and at high concentrations of calcium, whilst monocarbonate is stable over a wider range of concentrations, and suggested that it forms preferentially in systems containing alkalis. The reason for this was attributed to the common ion effect, which reduces the concentration of calcium, whilst increasing the concentration of sulfate, aluminate, and carbonate.

As mentioned in Ref. [5], several investigators have noted that the Fe/Ca ratio in the hydrate phases tends to be higher than that of the ferrite phase in the clinkers and have concluded that an iron (III) oxide gel or hydroxide is formed. Teoreanu et al. [17] concluded that the hydration products at ordinary temperatures included FH_3 , in agreement with Fukuhara et al. [18]. They based their conclusions on measurements of heat of hydration by conduction calorimetry and suggested that the hydration of C_4AF resulted in the formation of ettringite containing some iron [composition $\text{C}_3(\text{A}_{0.75}\text{F}_{0.25}) \cdot 3\text{CaSO}_4 \cdot 31\text{H}_2\text{O}$] and FH_3 . According to Taylor and Newbury [19], the tendency to form iron oxide gel or iron hydroxide may be related to the ability of Al^{3+} to migrate relatively easily through the paste, whilst Fe^{3+} , owing to its lower solubility, cannot and is therefore largely confined to the space originally occupied by the anhydrous ferrite phase.

After calculating the relative contents of hydrate phases in wt.%, the best available data on the densities of the hydrate phases can be used to calculate the relative contents in vol.% (e.g., in Refs. [5,20]).

3. Experimental

Three Portland cement pastes were examined: two white Portland cements with Bogue- C_3A contents of approximately 4% and 12%, and a grey Portland cement with a Bogue- C_3A content of 7%. The compositions of these cements are shown in Table 1.

Table 1
Composition of the Portland cements tested

Cement id.	SiO_2	Al_2O_3	Fe_2O_3	CaO	SO_3	Na_2O	K_2O	CO_2^a
WPC(4)	24.8	1.87	0.33	68.9	2.20	0.16	0.11	0.14
WPC(12)	23.6	4.49	0.21	65.9	2.38	0.03	0.20	0.72
OPC	21.0	4.90	3.64	65.1	3.00	0.30	0.41	0.08

Calculated Bogue composition

Cement id.	C_3S	C_2S	C_3A	C_4AF
WPC(4)	72.2	16.8	4.4	1.0
WPC(12)	51.7	28.6	11.5	0.6
OPC	59.1	15.6	6.8	11.1

^a Determined by DTG.

Table 2

Components in the w/s 0.70 'wet' mixes (i.e., the three cement pastes)

System id.	SiO_2	Al_2O_3	Fe_2O_3	CaO	SO_3	CO_2	H_2O
WPC(4)_070	24.62	1.86	0.33	68.70	2.18	0.56	70.00
WPC(12)_070	23.37	4.45	0.21	65.75	2.36	1.13	70.00
OPC_070	20.79	4.86	3.61	65.00	2.97	0.50	70.00

All the pastes were prepared at a w/p ratio of 0.70 after replacement of the cement by 1 wt.% finely ground calcite (specific surface area higher than $1000 \text{ m}^2/\text{kg}$). The powder was mixed for 5 min in a Hobart mixing machine before the addition of one third of the water and mixing for 3 min, followed by a further 3-min mixing with the remaining water. The pastes were cast in 2-cm^3 centrifuge tubes, sealed, and slowly rotated for 2 days to avoid bleeding. After demoulding, series of three 2-cm^3 specimens were placed in 12 ml decarbonated water, then sealed and stored at 20°C for 6 months, which was ample time for the hydrated cement to reach equilibrium and for the composition of the solution to remain constant. The solution is, to all extents and purposes, identical to the pore solution, albeit at a much lower alkali content, which is diluted by an order of magnitude.

After 6 months, the specimens were examined by EDS (at 15keV, 25 μA , and measuring time of 40 s/point, calibrated against relevant standards). The evaporable water content upon drying at 105°C was determined, followed by the determination of the loss of ignition at 1000°C .

4. Results

The compositions of the three cement pastes after the addition of limestone and water are given in Table 2.

Before calculating the relative contents of phases in each of the three hydrated cement pastes, analyses were per-

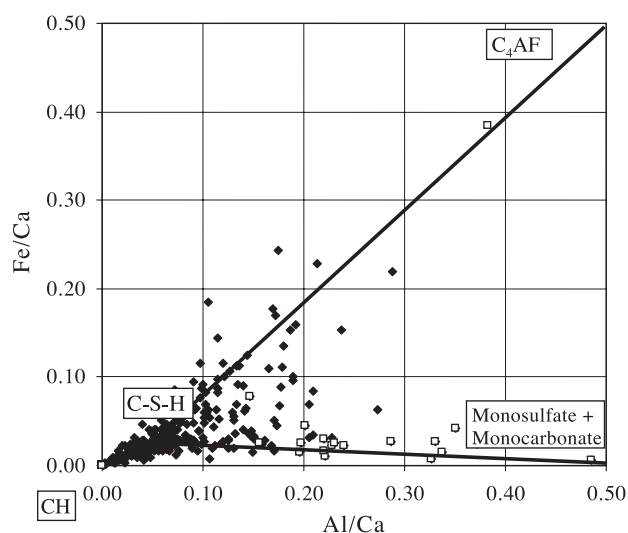


Fig. 2. 350 EDS analyses on OPC_070 plotted as Fe/Ca vs. Al/Ca (squares indicate plots with $\text{S}/\text{Ca} > 0.10$).

Table 3
Possible phase assemblages from the ternary subsystem in Fig. 1

1.	C ₄ AH ₁₃ , monosulfate, monocarbonate +	Phases in excess:
2.	monosulfate, ettringite, monocarbonate +	C-S-H, CH, FH ₃
3.	ettringite, calcite, monocarbonate +	and pore solution
4.	ettringite, calcite, gypsum +	

formed to determine the composition of the hydrate phases and the contents of the unreacted clinker. The hydration of the ferrite phase can be neglected in the case of the white Portland cements due to their very low iron content. Fig. 2 shows the results of 350 EDS individual spot analyses on the hydrated OPC pastes plotted as Fe/Ca versus Al/Ca (molar ratios).

Some plots show trends in the direction of the composition for C₄AF, indicating that not all of the ferrite has reacted. Some plots correspond to higher Fe/Ca molar ratios than the anhydrous phases (i.e., plots above the C-S-H–C₄AF tie line), indicating the presence of iron hydroxide intimately mixed with the other hydrates. The trends towards the monosulfate phase (i.e., squares in Fig. 2, which have a S/Ca > 0.10) indicate little or no iron in this phase.

The region bound by the C-S-H–monosulfate/monocarbonate–C₄AF tie lines in Fig. 2 can be regarded as a type of phase diagram, with each plot representing the chemical composition of a volume of paste, the size of which depends on the conditions of analysis on the SEM (generally a few μm^3). All the plots within this region can be projected onto the C-S-H–C₄AF tie line by tracing a line from the monosulfate composition through each plot to where it intersects the tie line. The average Fe/Ca ratio of the mixture of C-S-H and C₄AF can then be used to calculate the volume ratio of C-S-H to C₄AF. The composition of the C-S-H used here assumed some solid solution of iron corresponding to a Fe/Ca ratio of 0.02 (see Fig. 2). For the OPC paste examined, the average Fe/Ca ratio was 0.405, corresponding to a C₄AF/C-S-H volume ratio of approximately 0.03, equivalent to a C₄AF content of 2.20% by weight of solid phases. This corresponds to a degree of hydration for C₄AF of approximately 75%, which is in agreement with the data in

Refs. [5,20]. This was confirmed by point counting of a polished section (2600 counts), which gave a C₄AF content of 0.7 vol.% of the total paste.

Refs. [5,20] reported a degree of reaction of the belite phase after 6 months hydration of approximately 80%. The alite and aluminate phases are almost completely hydrated [5], and therefore, the degree of hydration of these is assumed to be 95%. For the systems examined, the overall degree of hydration is estimated to be 88–92%, based on the Bogue composition in Table 1. Parrott et al. [21] found the degree of hydration of a white Portland cement [the same as WPC(4) in the present investigation] at 100 days of maturity to be approximately 90% for a w/s ratio of 0.71 by QXRD analysis. They also carried out measurements on an ordinary Portland cement with similar composition and properties to the OPC cement in this investigation and found a degree of hydration of approximately 85% at a maturity of 100 days.

According to the ternary subsystem in Fig. 1, four assemblages are possible, as shown in Table 3. The relative compositions and densities of the hydrate phases are given in Table 4. Only one of these assemblages is possible for each of the cements when solving the 7 × 7 simultaneous equations.

The assemblages predicted from the cement compositions in Table 2 are shown in Table 5, with the relative contents of phases given in wt.% of the water-saturated system. Note that the amount of pore solution assumes water-saturated conditions, in which the volume produced from chemical shrinkage is taken up by the absorption of additional water.

The evaporable water is estimated as the sum of pore solution and evaporable water in the C-S-H in mass percent, which is considered to be weakly bound water that evaporates on drying at 105 °C (in, e.g., Refs. [5,11]). The chemically bound water in the other phases is assumed to be nonevaporable water, which is not entirely correct, as particularly the ettringite and hydroxy-AFm phases and, to a lower extent, other AFm phases will lose considerable amounts of water on drying at 105 °C [5]. For the cements

Table 4
Phase compositions and densities

Component phase	SiO ₂	Al ₂ O ₃	Fe ₂ O ₃	CaO	SO ₃	CO ₂	H ₂ O	Density [g/cm ³]
C-S-H	25.24	1.49		41.23	1.77		30.27	1.95–2.45
CH				75.69			24.31	2.24
FH ₃			89.76				10.24	4.28
Pore solution							100.0	1.00
Gypsum				32.57	46.50		20.93	2.32
Ettringite		8.12		26.81	19.14		45.93	1.77
Monosulfate		16.38		36.03	12.86		34.73	2.01
C ₄ AH ₁₃		18.19		40.02			41.79	2.05
Monocarbonate		17.94		39.46		7.74	34.86	2.01
Calcite				56.03		43.97		2.72

Data from Refs. [5,20].

Table 5
Phase contents calculated for each cement, in wt.%, to water saturated paste

	WPC(4)_070	WPC(12)_070	OPC_070
Assemblage number in Table 3	3	3	2
C _{1.75} SH ₄	50.8	47.2	42.9
CH	19.2	14.6	16.5
FH ₃	0.2	0.1	1.8
Pore solution	22.3	21.4	22.7
Monosulfate	–	–	6.3
Ettringite	1.9	2.8	0.8
Monocarbonate	0.4	8.4	3.7
Calcite	0.7	0.1	–
C ₃ S	1.8	1.2	1.5
C ₂ S	2.6	3.9	2.1
C ₃ A	0.1	0.3	0.2
C ₄ AF	0.1	0.1	1.6
Density of C-S-H [g/cm ³]	2.11	2.09	2.10
Evaporable water in C-S-H [wt.%]	18.5	19.0	19.0
Chemical shrinkage [ml/100g cement]	5.8 (5.5–6.0)	5.7 (5.5–6.0)	5.9 (5.5–6.0)
Vol.% capillary porosity	38.5	36.9	39.1
Evaporable water [wt.% to sat. paste]	31.5 (31.0)	30.7 (30.5)	31.0 (31.0)
LOI [wt.% to dry paste]	18.8 (18.6)	20.6 (20.4)	20.6 (20.8)

studied here, however, this does not affect the above assumption because none of the pastes contain hydroxy-AFm, and the amount of ettringite is very low. The loss of ignition is estimated by adding all the nonevaporable water in the system to the amount of CO₂, which is released on ignition at 1000 °C.

The density of the C-S-H phase and its content of evaporable water were the uncertain input data used for the calculations. These properties have a major effect on the chemical shrinkage of the paste and the loss of ignition, respectively, allowing, therefore, adjusting them separately. The evaporable water content of the paste is affected by both properties. Table 5 shows the actual density that gave the best fit for the predicted parameters (chemical shrinkage, loss of ignition, and evaporable water) and those determined experimentally (also included in the table, in parenthesis). Note that the chemical shrinkage measurements were not carried out in this study but were determined elsewhere on similar cements [21,22]. The density of the C-S-H is approximately 2.10 g/cm³, and the evaporable water content of the C-S-H is approximately 19%. No significant difference was observed between the white and grey cements, which suggests that the densities used for the phases are correct, and the assumption that all iron not incorporated in the C-S-H is found as an iron hydroxide is valid.

Fig. 3 shows 1500 EDS plots for S/Ca versus Al/Ca determined for the hydrated cement WPC(4)_070. A large number of measurements were needed, owing to the low contents of alumina and sulfur in this cement. Most of the AFm phases and ettringite are intimately mixed with the C-

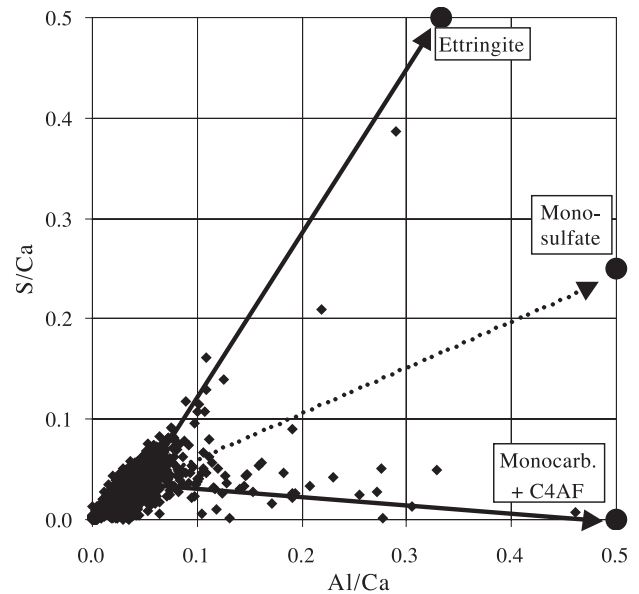


Fig. 3. 1500 EDS plots from WPC(4)_070, as S/Ca vs. Al/Ca.

S-H phase. However, the plots clearly show the presence of ettringite and confirm the absence of monosulfate. The trend towards the point (Al/Ca,S/Ca)=(0.5,0.0) indicates the presence of either C₄AF and/or an AFm phase without sulphur. Given the absence of C₄AF and an aluminate content insufficient to form the hydroxy-Afm phase, it is concluded that these plots must represent a mixture of monocarbonate and C-S-H. Observations on the ESEM also confirmed that a considerable amount of the calcite remained as a stable phase, as predicted by the model. The calcite had fully reacted in the pastes prepared from the high-aluminate cements WPC(12)_070 and OPC_070, again, as predicted by the model.

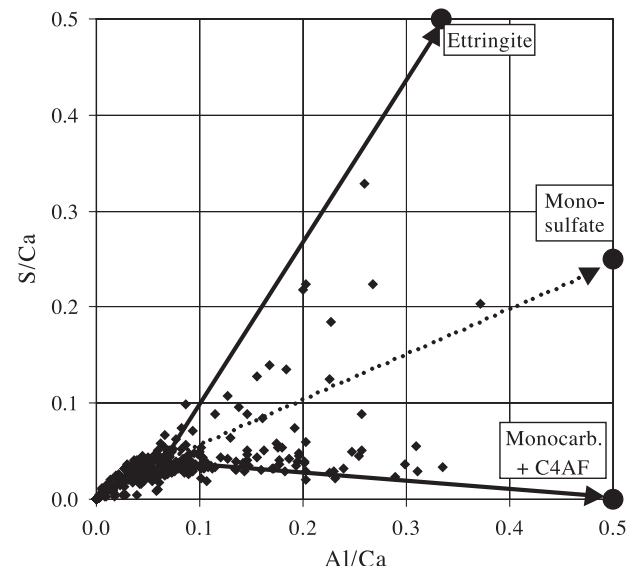


Fig. 4. 350 EDS plots from WPC(12)_070, as S/Ca vs. Al/Ca.

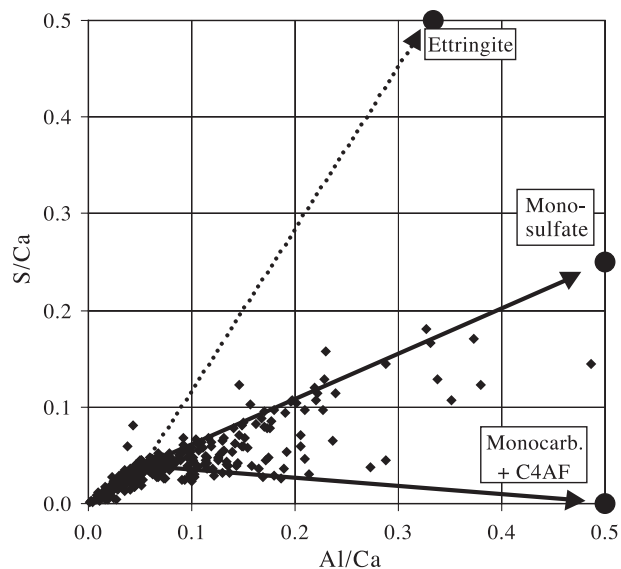


Fig. 5. 350 EDS plots form OPC_070, as S/Ca vs. Al/Ca.

The hydrated cement WPC(12)_070 has a high content of alumina and about twice as much CO_2 as the two other cements (see Table 2). The composition of the paste is close to the monocarbonate–ettringite tie line on Fig. 1, and the amount of calcite or monosulfate is therefore low. The dominant aluminate-containing phase in this hydrated cement is monocarbonate, which is confirmed by the plots in Fig. 4. The plots above the C-S-H–monosulfate tie line indicate the presence of ettringite.

Fig. 5 shows 350 EDS plots for the hydrated cement OPC_070 and confirms that the stable phases here are monocarbonate and monosulfate. No clear tendency towards ettringite is observed, but a low content was also predicted by the model. It should be noted that some of the plots close to the C-S-H–monocarbonate tie line include some of the unreacted C_4AF clinker phase.

5. Conclusion

The accuracy of a method based on the phase rule for predicting the phase assemblage and calculating the relative contents of phases was tested by EDS analysis. The stability and relative contents of monosulfate, monocarbonate, and ettringite are consistent with the predictions for each of the three cements tested. Composition of the C-S-H was $\text{C}_{1.75}\text{SH}_4$ with $\text{Al}/\text{Ca}=0.04$, $\text{S}/\text{Ca}=0.03$, and $\text{Fe}/\text{Ca}=0.02$ (only in the grey cement).

The results indicated that approximately 3/4 of the ferrite phase had reacted after 6 months, and apart from some solid solution of iron and aluminium in the C-S-H phase, the aluminate exclusively formed AFm phases and ettringite. Also, all the available iron formed a hydrous iron phase, presumably FH_3 .

The model was also used to calculate the capillary porosity. The density of the C-S-H phase, as well as its content of evaporable water, needed in this calculation was adjusted until agreement was reached between the values for chemical shrinkage, loss of ignition, and evaporable water content predicted by the model and those determined experimentally. The C-S-H phase densities determined in this way were 2.11, 2.09, 2.10 g/cm^3 in the three cement pastes studied, suggesting the true density of the C-S-H in water-saturated Portland cement to be approximately 2.10 g/cm^3 . The evaporable water content of the water-saturated C-S-H was 19 wt. %.

References

- [1] T.C. Powers, T.L. Brownyard, Studies of the physical properties of hardened portland cement paste, *J. ACI* 18 (8) (1947) (Part 9) 971–992.
- [2] D.P. Bentz, Three-dimensional computer simulation of Portland cement hydration and microstructure development, *J. Am. Ceram. Soc.* 80 (1997) 3–21.
- [3] D.P. Bentz, CEMHYD3D: a three-dimensional cement hydration and microstructure development modeling package. Version 2.0, Internal report NISTIR 6485, Building and Fire Research Laboratory, NIST, Gaithersburg, 2000.
- [4] K. van Breugel, Simulation of Hydration and Formation of Structure in Hardening Cement-Based Materials, 2nd ed., Technical University of Delft, Delft, 1997.
- [5] H.F.W. Taylor, Cement Chemistry, 2nd ed., Thomas Telford Services, London, 1997.
- [6] D. Herfort, I.A. Juel, The mineralogy of sulfate and sea water attack on concrete interpreted from EPMA analysis, Proceedings of the 23rd International Conference on Cement Microscopy, Albuquerque, New Mexico, 2001.
- [7] I.A. Juel, D. Herfort, The mineralogy of chloride attack on concrete containing limestone filler, Proceedings of the 24th International Conference on Cement Microscopy, San Diego, California, 2002.
- [8] E.P. Nielsen, D. Herfort, M.R. Geiker, R.D. Hooton, Effect of solid solutions of AFm phases on chloride binding, Proceedings of the 11th International Congress on the Chemistry of Cement, Durban, South Africa, 2003.
- [9] F.P. Glasser, Application of the phase rule to cement chemistry, in: A.M. Alper (Ed.), Chapter 5 in *Refractory Materials Volume 6-II*, Academic Press, New York, 1970, 147–190.
- [10] A. Putnis, J.D.C. McConnell, Principles of Mineral Behaviour, Elsevier, New York, 1980.
- [11] S.-Y. Hong, F.P. Glasser, Alkali binding in cement pastes: Part I. The C-S-H phase, *Cem. Concr. Res.* 29 (1999) 1893–1903.
- [12] S.-Y. Hong, F.P. Glasser, Alkali sorption by C-S-H and C-A-S-H gels: Part II. Role of alumina, *Cem. Concr. Res.* 32 (2002) 1101–1111.
- [13] E.P. Nielsen, D. Herfort, M.R. Geiker, Binding of chlorides and alkalis in Portland cement systems, *Cem. Concr. Res.* 35 (2004) 117–123, doi:10.1016/j.cemconres.2004.05.026.
- [14] C. Famy, K.L. Scrivener, A. Atkinson, A.R. Brough, Effects of an early or a late heat treatment on the microstructure and composition of inner C-S-H products of Portland cement mortars, *Cem. Concr. Res.* 32 (2002) 269–278.
- [15] D. Damidot, F.P. Glasser, Thermodynamic investigation of the $\text{CaO}-\text{Al}_2\text{O}_3-\text{CaSO}_4-\text{CaCO}_3-\text{H}_2\text{O}$, *Adv. Cem. Res.* 27 (1995) 129–134.
- [16] H.-J. Kuzel, H. Pöllmann, Hydration of C_3A in the presence of $\text{Ca}(\text{OH})_2$, $\text{CaSO}_4 \cdot 2\text{H}_2\text{O}$ and CaCO_3 , *Cem. Concr. Res.* 21 (1991) 885–895.
- [17] I. Teoreanu, G. Filoti, C. Hritcu, L. Bucea, V. Spânu, S. Ciocanel, M. Ivăscu, Interaction mechanism of $2\text{CaO} \cdot \text{Fe}_2\text{O}_3$ and $4\text{CaO} \cdot \text{Al}_2\text{O}_3$.

- Fe_2O_3 with water, at various pressures and temperatures, *II Cemento* 76 (1979) 19–28.
- [18] M. Fukuhara, S. Goto, K. Asaga, M. Daimon, R. Kondo, Mechanisms of C_4AF hydration with gypsum, *Cem. Concr. Res.* 11 (1981) 407–414.
- [19] H.F.W. Taylor, D.E. Newbury, An electron microprobe study of a mature cement paste, *Cem. Concr. Res.* 14 (1984) 565–573.
- [20] F.M. Lea, *The Chemistry of Cement and Concrete*, 3rd ed., Edward Arnold Press, London, 1970.
- [21] L.J. Parrott, M. Geiker, W. Gutteridge, D. Killoh, Monitoring Portland cement hydration: comparison of methods, *Cem. Concr. Res.* 20 (1990) 919–926.
- [22] M.R. Geiker, Studies of Portland cement hydration by measurements of chemical shrinkage and a systematic evaluation of hydration curves by means of the dispersion model, doctoral Thesis, Institute of Mineral Industry, Technical University of Denmark, Lyngby, 1983.